

Preventing Structural Rearrangements on Battery Cycling: A First Principles Investigation of the Effect of Dopants on the Migration Barriers in Layered $\text{Li}_{0.5}\text{MnO}_2$

Ieuan D. Seymour, David J. Wales and Clare P. Grey*

Department of Chemistry, University of Cambridge, Cambridge, CB2 1EW, United Kingdom

SUPPLEMENTARY INFORMATION

The changes in the local bonding around a Mn^{4+} ion in a MnO_6 octahedral environment with a M^{3+} dopant (Al^{3+} , Cr^{3+} , Ga^{3+} , Fe^{3+} , Sc^{3+} and In^{3+}) in the first cation coordination sphere was investigated. The variation in the local Mn^{4+} -O bond lengths are shown in Table S1 for the doped cells and the undoped, $\text{Li}_{0.5}\text{MnO}_2$ (Mn) cell.

Table S1: Variation in local bond length with the inclusion of a metal, M^{3+} , dopant in the ordered Li and vacancy chain structure of $\text{Li}_{0.5}\text{MnO}_2$. The Mn^{4+} -O bond length of the 1st nearest neighbor octahedral Mn^{4+} site are shown. The positive Jahn Teller distortion of the neighboring Mn^{3+} species results in 4 shortened bonds and 2 lengthened bonds for all species. Average bond length = $1/3 \times \text{long} + 2/3 \times \text{short}$

Dopant	Ionic Radius (Å)	1 st nn Mn^{4+} -O Bond Length (Å)		
		Short	Long	Average
Mn	0.645	1.921	1.949	1.931
Al	0.535	1.922	1.958	1.934
Cr	0.615	1.920	1.957	1.933
Ga	0.62	1.922	1.954	1.933
Fe	0.645	1.921	1.955	1.933
Sc	0.745	1.922	1.953	1.932
In	0.8	1.923	1.951	1.932

The volume of the Li tetrahedral site in configuration *b* for all the first nearest neighbor doped structures was found to be inversely proportional to the ionic radius of the M^{3+} dopant, as is shown in Figure S1.

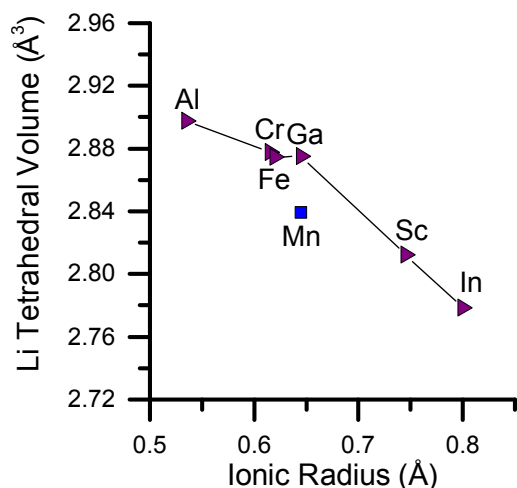


Figure S1: The variation in the Li tetrahedral volume with the ionic radius of a dopant in the 1st nearest neighbor coordination to Mn³⁺ dopant in the vacancy ordered structure of Li_{0.5}MnO₂ with one tetrahedral Li (configuration *b*), is shown with filled triangles. The tetrahedral volume for Li in undoped Li_{0.5}MnO₂ (Mn) reproduced from ref 1 is shown with a square.

The migration of Cr in the Li_{0.5}MnO₂ structure was found to occur in a two stage process involving the migration of Cr from an octahedral (CrO₆) to a square pyramidal (CrO₅) site, followed by migration from the square pyramidal site to a tetrahedral (CrO₄) site. The transition state for the square pyramidal to tetrahedral migration is shown in Figure S2.

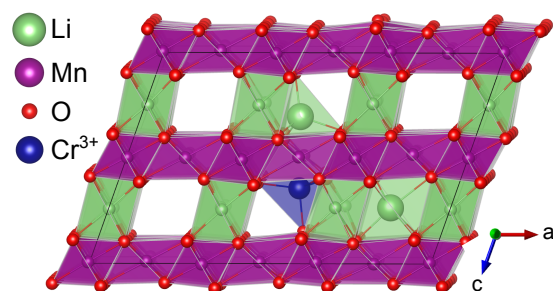


Figure S2: A schematic representation of the transition state structure for Cr³⁺ diffusion between a square pyramidal, CrO₅ site and a tetrahedral, CrO₄, site in the structure of Li_{0.5}MnO₂. The diffusing species are enlarged for clarity.

The oxidation state of Cr during the octahedral → square pyramidal → tetrahedral migration process was monitored from the integrated differential spin density around Cr, as is shown in Figure S3. A sphere radius of 1.8 Å was used around the Cr site for the integration.

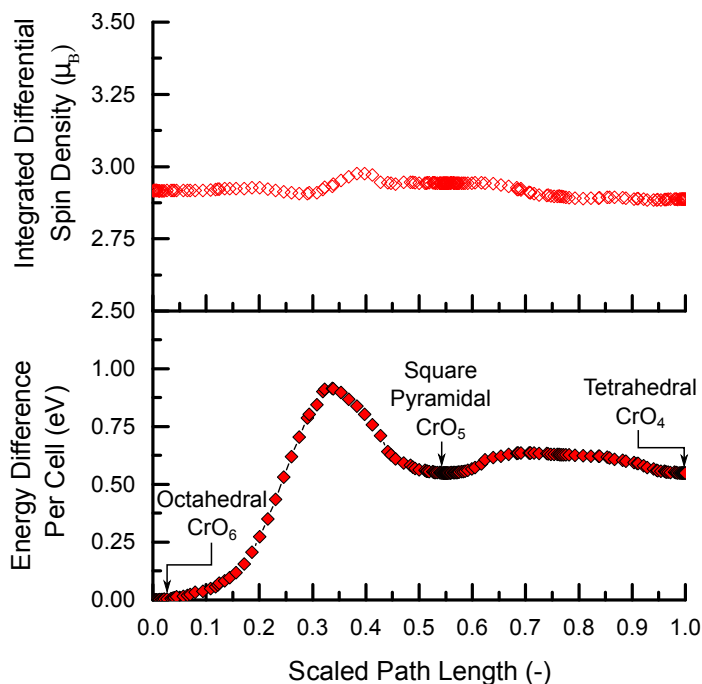


Figure S3: (Bottom) Energy along the migration pathway of a Cr^{3+} dopants from the octahedral \rightarrow square pyramidal \rightarrow tetrahedral sites within the structure of $\text{Li}_{0.5}\text{MnO}_2$. (Top) Integrated spin density on the diffusing Cr species.

In Figure S3, the diffusing Cr ion maintains a spin of approximately $2.9 \mu_B$ throughout the migration process, corresponding to a charge state of Cr^{3+} .

The diffusion of In^{3+} and Sc^{3+} from octahedral sites in the Mn layer (configuration *c* in Figure 1 of the main text) to tetrahedral sites in the Li layer (configuration *f* in Figure 1 of the main text), was found to occur simultaneously with the migration of an octahedral Li from the ordered chain to a tetrahedral site above the dopant. The local minima and transition state structures are shown in Figure S4.

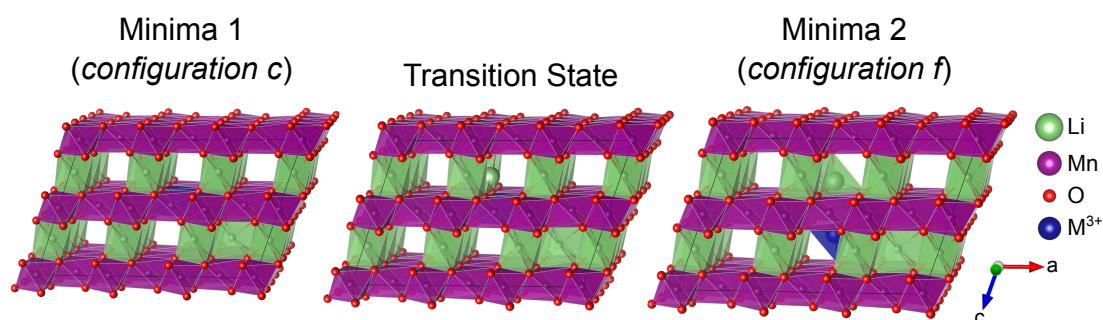


Figure S4: A schematic representation of cooperative migration pathway for M^{3+} (Sc and In) dopants and Li from octahedral sites (configuration *c*) to tetrahedral sites (configuration *f*) in the structure of $\text{Li}_{0.5}\text{MnO}_2$. The diffusing species are enlarged for clarity.

REFERENCES

- (1) Seymour, I. D.; Chakraborty, S.; Middlemiss, D. S.; Wales, D. J.; Grey, C. P. Mapping Structural Changes In Electrode Materials: Application Of The Hybrid Eigenvector-Following Density Functional Theory (DFT) Method To Layered $\text{Li}_{0.5}\text{MnO}_2$. *Chem. Mater.* 2015, 27, 5550–5561.